Available online at www.sciencedirect.com

SciVerse ScienceDirect

Ceramics International 39 (2013) 2383–2387

CERAMICS INTERNATIONAL

www.elsevier.com/locate/ceramint

Photoluminescence properties of Eu^{2+}-activated $BaCa_2Al_8O_{15}$ nanophosphors

Donglei Wei[a,b], Lin Qin[a], Yanlin Huang[a,*], Hyo Jin Seo[c,**]

[a]*College of Chemistry, Chemical Engineering and Materials Science, Soochow University, Suzhou 215123, China*
[b]*Interdisciplinary program of LED and Solid State Lighting Engineering, Pukyong National University, Busan 608-737, Republic of Korea*
[c]*Department of Physics, Pukyong National University, Busan 608-737, Republic of Korea*

Received 31 July 2012; received in revised form 30 August 2012; accepted 30 August 2012
Available online 4 September 2012

Abstract

A new blue-emitting nanophosphor of Eu^{2+}-activated $BaCa_2Al_8O_{15}$ was synthesized by the Pechini method. The phosphors were investigated by X-ray powder diffraction (XRD) measurement and confirmed to be a pure crystalline phase of $BaCa_2Al_8O_{15}$. The photoluminescence excitation and emission spectra, the luminescence decay and the color coordinates were taken to investigate the luminescence characteristics. The dependence of luminescence intensities $BaCa_2Al_8O_{15}$:Eu^{2+} on the doping concentrations was investigated. This nanophosphor can be efficiently excited by UV light and presents bright blue luminescence. Under the same conditions, the light yield of $BaCa_2Al_8O_{15}$:Eu^{2+} is about 1.2 times higher than that of blue-emitting phosphor $BaMgAl_{10}O_{17}$:Eu^{2+}. Eu^{2+}-activated $BaCa_2Al_8O_{15}$ nanophosphor exhibits the long-lasting phosphorescence, which was analyzed by measuring the afterglow decay curves. The co-doped Eu^{3+} ions and some defects were suggested to be the possible trap-centers.

Keywords: Eu^{2+} ions; Photoluminescence; Inorganic compounds; Long-lasting phosphorescence

1. Introduction

Rare-earth ions (RE) doped inorganic phosphors have many applications in high-performance displays and devices such as plasma display devices (PDPs), field emission displays (FEDs), cathode ray tubes (CRTs), electroluminescent displays (ELs), laser generation apparatus, and white light-emitting diodes (W-LEDs) [1–5]. Up to now, many materials have been studied in order to develop the potential phosphors. Among them, the aluminates are well known phosphor host materials, which have been intensively studied for their luminescent properties [6–8].

Phosphors based on Eu^{2+}-doped alkaline-earth aluminates have been widely investigated due to their various crystal structures, high chemical stability, high brightness and long lasting photoluminescence [9]. Usually the crystal field environments have great influence on 5d–4f transition of the Eu^{2+} ions, so the emission wavelengths of Eu^{2+}-doped strontium aluminates are strongly dependent on the host crystal structure. In the past years, the efficient blue-emitting phosphors based on Eu^{2+}-activated aluminates have been well developed, e.g., $Ca_3ZnAl_4O_{10}$:Eu^{2+} (445 nm) [10], $Sr_4Al_{14}O_{25}$:Eu^{2+} (490 nm) [11], $SrAl_2O_4$ (520 nm) [12], $Sr_2Al_6O_{11}$ (460 nm) [13], $SrAl_{12}O_{19}$ (400 nm) [14] and $BaMgAl_{10}O_{17}$:Eu^{2+} (450 nm, BAM:Eu^{2+}) [15], especially BAM:Eu^{2+} has been widely used in fluorescent lamps and plasma display panels (PDPs) due to its high luminescence efficiency and good color chromaticity.

Usually, Eu^{2+}-doped aluminate phosphors are prepared at high temperatures in a reduction atmosphere in order to get the required host matrices, consequently some defects in the crystal lattices can be inherently created in inhomogeneous distributions. The electron- and hole-traps originated from the defects can provide a recombination of electrons with exciting Eu^{2+} ions. This process usually can induce long lasting phosphorescence [16]. Therefore, it is a common phenomenon for a Eu^{2+}-doped alkaline-earth

*Corresponding author.
**Corresponding author.
E-mail addresses: huang@suda.edu.cn (Y. Huang), hjseo@pknu.ac.kr (H.J. Seo).

0272-8842/$ - see front matter © 2012 Elsevier Ltd and Techna Group S.r.l. All rights reserved.
http://dx.doi.org/10.1016/j.ceramint.2012.08.090

aluminate to present long lasting phosphorescence. In particular, Eu^{2+}-doped $MAl_2O_4:Eu^{2+}$ (M=Ca, Ba, and Sr) have attracted great interest due to their high efficiency in long-afterglow phosphorescence and the potential application areas include emergency signs, textile fibers, display devices and optical memory units [17–22].

In this work Eu^{2+}-activated $BaCa_2Al_8O_{15}$ blue-emitting nanophosphors were synthesized by the Pechini method. The structure was investigated by powder X-ray diffraction (XRD) measurement. The excitation and emission spectra, decay curves, and SEM images were measured. The photoluminescence properties of Eu^{2+}-activated $BaCa_2Al_8O_{15}$ were compared with those of the well-known blue-emitting phosphor BAM:Eu^{2+}. In addition, the long lasting phosphorescence in $BaCa_2Al_8O_{15}:Eu^{2+}$ phosphor was investigated by the afterglow decay curves and time-resolved emission spectra.

2. Experimental

Eu^{2+}-activated $BaCa_2Al_8O_{15}:xEu^{2+}$ (x=0.01–0.07) powder nanophosphors were prepared by the Pechini method. The raw materials were stoichiometric mixture of reagent grade barium nitrate ($Ba(NO_3)_3\cdot 4H_2O$), calcium nitrate ($Ca(NO_3)_3\cdot 4H_2O$), aluminum nitrate ($Al(NO_3)_2\cdot 9H_2O$), and europium oxide Eu_2O_3. First, Eu_2O_3 was dissolved in the diluted HNO_3; then, the starting materials were dissolved in an aqueous solution of citric acid (99.5%) under constant stirring at 80 °C until the solution became clear. The molar ratio of the citric acid to total cation ions was 2:1. The ethylene glycol (the ethylene glycol and citric acid in a 4:1 M ratio) was added to promote the polymerization of the metal citrates by the polyesterification reaction. And then, the solutions were slowly heated to 100 °C and kept at this temperature for 2 h. The obtained gels were put into an oven to dry at 150 °C for 10 h, and the porous solid resins were produced; then solid resins were treated in air at 1000 °C for 8 h. After that, the sample was thoroughly mixed and heated at 1300 °C for 10 h in a covered crucible imbedded in the active carbon.

The XRD pattern was collected on a Rigaku D/Max-2000 diffractometer operating at 40 kV and 30 mA with the Bragg–Brentano geometry by using Cu Kα radiation (λ = 1.5418 Å). The optical excitation and emission spectra were recorded by a Perkin–Elmer LS-50B luminescence spectrometer and a Hitachi F-4500 fluorescence spectrophotometer. To measure the luminescence decays, the luminescence under the excitation of the third harmonic (355 nm) of a pulsed Nd:YAG laser was dispersed by a 75 cm monochromator (Acton Research Corporation Pro-750). The decay curves were recorded from a digital oscilloscope (LeCloy 9301), in which the signal was fed from PMT (Hamamatsu R928).

3. Results and discussion

3.1. The phase formation and crystal structure

Fig. 1 shows the X-ray powder diffraction patterns of 1.0, 3.0 and 5.0 mol% Eu^{2+}-doped $BaCa_2Al_8O_{15}$ prepared by the Pechini method. The patterns were compared with the PDF2 Card no. 15-0342 ($BaCa_2Al_8O_{15}$) selected from the International Centre for Diffraction Data (ICDD) database. By a comparison between them, the positions and relative intensities of the main peaks in the samples well match the standard card. No impurity lines were observed, and all the reflections could be well indexed to a single phase $BaCa_2Al_8O_{15}$.

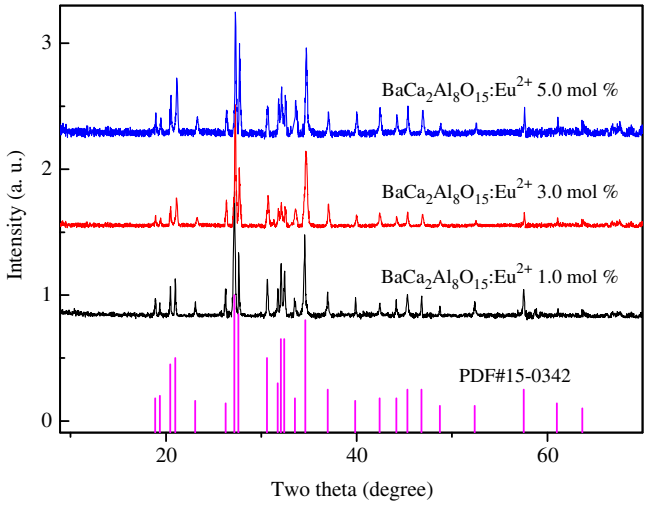

Fig. 1. XRD patterns of $BaCa_2Al_8O_{15}:xEu^{2+}$ (x=0.01, 0.03, and 0.05) nanophosphors compared with the corresponding PDF2 Card no. 15-0342.

Fig. 2 shows the SEM micrograph of $BaCa_2Al_8O_{15}:0.05Eu^{2+}$ nanophosphor. The sample has small ball-like nano-particles. All the particles are lightly aggregated and have an average particle size of about 200–500 nm.

3.2. The excitation and emission spectra

The typical photoluminescence excitation and emission spectra of $BaCa_2Al_8O_{15}:0.05Eu^{2+}$ nanophosphor are presented in Fig. 3, which are compared with the well-known blue-emitting phosphor BAM:Eu^{2+}. The excitation spectrum of $BaCa_2Al_8O_{15}:xEu^{2+}$ (x=0.05) (Fig. 3a) monitored at 440 nm consists of the broad absorption bands from 250 nm to 410 nm with the maximum wavelength 360 nm, which is ascribed to the 4f–5d transitions of Eu^{2+} ions. BAM:Eu^{2+} shows the main excitation at 254 and 330 nm bands attributed to 4f–5d transitions of Eu^{2+} ions (Fig. 3b).

The emission spectrum of $BaCa_2Al_8O_{15}:xEu^{2+}$ (x=0.05) (Fig. 3c) under the 365 nm excitation shows bright blue luminescence at 440 nm with a full width at half maximum (FWHM) 65 nm. This blue emission band originates from the allowed $4f^65d^1\rightarrow 4f^7(^8S_{7/2})$ electric dipole transition of Eu^{2+} ions. The corresponding Stokes shift of $BaCa_2Al_8O_{15}:0.05Eu^{2+}$ can be calculated to be 4600 cm^{-1}. In the emission spectrum of BAM:Eu^{2+}, one emission band peaking at 450 nm with a FWHM 58 nm (Fig. 3d) is observed from the $4f^65d\rightarrow 4f^7$ ($^8S_{7/2}$) transitions in Eu^{2+} ions. The ratio of luminescence intensity of $BaCa_2Al_8O_{15}:xEu^{2+}$ (x=0.05) to that of BAM:Eu^{2+} is 1.2:1.

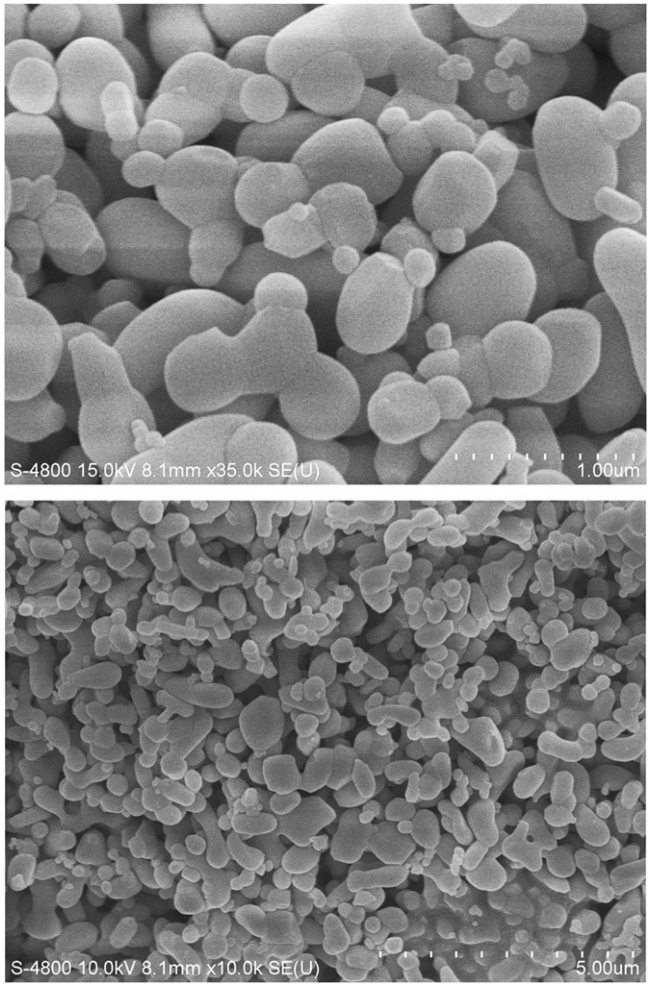

Fig. 2. Typical SEM micrographies of $BaCa_2Al_8O_{15}$:xEu^{2+} (x=0.05) nano-particles prepared by the Pechini method.

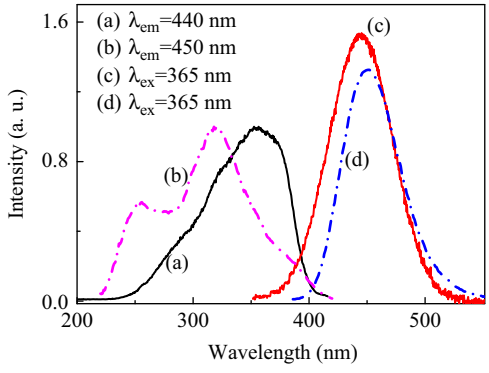

Fig. 3. (a) The excitation spectrum of 440 nm emission in $BaCa_2Al_8O_{15}$:xEu^{2+} (x=0.05), (b) the excitation spectrum of 450 nm emission of BAM:Eu^{2+}, (c) the emission spectrum in $BaCa_2Al_8O_{15}$:xEu^{2+} (x=0.05), and (d) the emission spectrum of BAM:Eu^{2+}. The two excitation spectra were normalized in the same intensity, and the two emissions were shown in the absolute experimental intensities measured under the same conditions by the excitation of a 365 nm-UV lamp.

Fig. 4 shows the concentration dependence of the emission spectra of $BaCa_2Al_8O_{15}$:xEu^{2+} (x=0.01–0.07). The emission intensity increases with Eu^{2+}-concentration increasing until a

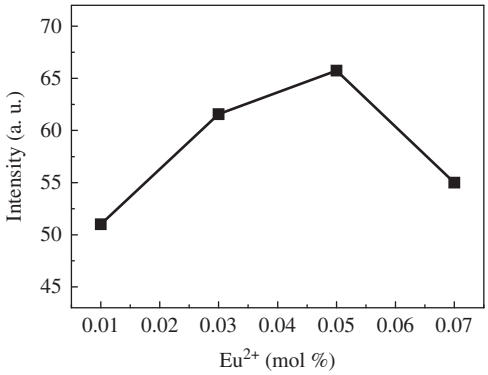

Fig. 4. Dependence of the luminescence intensity on the Eu^{2+} doping concentrations in $BaCa_2Al_8O_{15}$:xEu^{2+} (x=0.01–0.07).

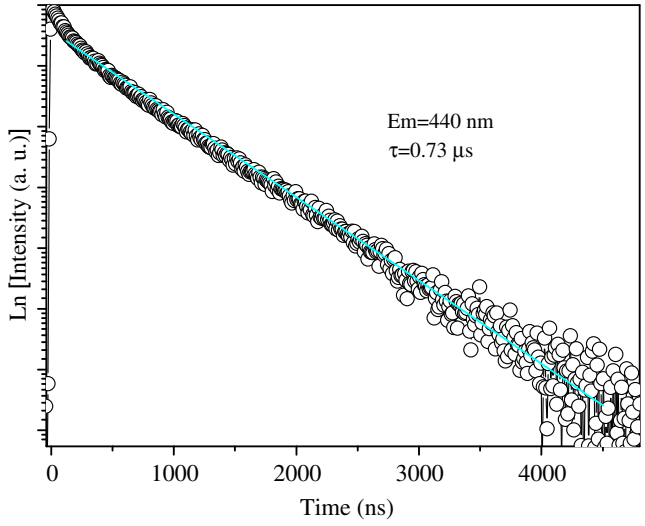

Fig. 5. Luminescence decay curve of $BaCa_2Al_8O_{15}$:Eu^{2+} 5.0 mol% under the excitation of 355 nm pulsed YAG:Nd^{3+}.

maximum intensity (x=0.05) reaches the top, and then it decreases due to the concentration quenching. The critical quenching concentration (x_c) of Eu^{2+} in $BaCa_2Al_8O_{15}$ is defined to be about 5.0 mol%. In addition, under 365 nm excitation, the phosphors show similar blue emission profiles peaked at 440 nm. The emission position and the spectrum shape have no obvious changes with the increase of Eu^{2+} concentration.

The CIE (Commission International de l'Eclairage 1931) chromaticity coordinate of $BaCa_2Al_8O_{15}$:xEu^{2+} (x=0.01–0.07) was calculated to be (x=0.142, y=0.07) in the blue region. The CIE values of the blue-emitting phosphor BAM:Eu^{2+} were reported to be (x=0.147, y=0.063) [23]. It can be seen that the CIE coordinates of $BaCa_2Al_8O_{15}$:xEu^{2+} well match the National Television System Committee (NTSC) blue standard (x=0.14, y=0.08) [24].

The decay curve $BaCa_2Al_8O_{15}$:0.05Eu^{2+} is shown in Fig. 5, which can be fitted in an exponential equation with a lifetime of 0.73 μs. The luminescence lifetimes of other samples $BaCa_2Al_8O_{15}$:xEu^{2+} have similar values: 0.76 μs (x=0.01), 0.78 μs (x=0.03), 0.72 μs (x=0.07),

3.3. Afterglow decay curves of the phosphors

The obvious characteristic of $BaCa_2Al_8O_{15}$:xEu^{2+} (x=0.01–0.07) nanophosphors is that the afterglow luminescence can be obviously seen by naked eyes after the removal of the excitation source UV lamp (254 nm and 365 nm). Fig. 6 shows the afterglow decay curves by monitoring the total emission after the UV—ultraviolet lamp has been removed.

The results show that the luminescence afterglow is enhanced with increasing Eu^{2+} doping. All the samples show a rapid initial decay and subsequent long-lasting phosphorescence, which can be analyzed by the following empirical equation [25]:

$$I = I_0 + A_1\exp(-t/\tau_1) + A_2\exp(-t/\tau_2) \quad (1)$$

where I represents the phosphorescence intensity at any time 't' after stopping the excitation of UV light, $A_1$and A_2 are constants, and τ_1 and τ_2 are the decay constants, which determine the decay rate for the rapid, the slow exponential decay components, respectively. The fitting result values of τ_1 and τ_2 parameters are listed in Table 1.

The results indicate that the decay has two different components: initial fast decay and the long decay afterglow. It is probably due to the existence of traps with appropriate depth. The electrons and holes produced by UV excitation move back to Eu^{2+} sites through thermal hopping and tunneling, and recombine radiatively at Eu^{2+} sites in the lattices. Such kind of afterglow was also reported in Eu^{2+}-doped silicates (e.g., Ba_2SiO_4 and Ba_3SiO_5 crystals [26]), and phosphates (e.g., $LiBaPO_4$:Eu^{2+} [27]).

In $BaCa_2Al_8O_{15}$:xEu^{2+} (x=0.01–0.07) nanophosphors, the luminescence from Eu^{3+} ions can be also distinctly

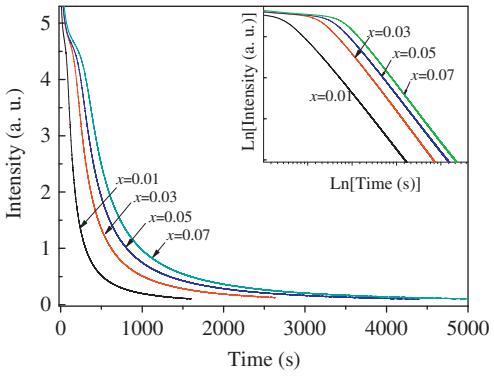

Fig. 6. Experimental afterglow curves of $BaCa_2Al_8O_{15}$:xEu^{2+} (x=0.01–0.07) nano-phosphors.

Table 1
Parameters of afterglow calculated from multiple exponential fit for the decay curves of $BaCa_2Al_8O_{15}$:xEu^{2+} (x=0.01–0.07) nanophosphors.

x	0.01	0.03	0.05	0.07
τ_1 (s)	85	165	218	262
τ_2 (s)	366	656	932	1076

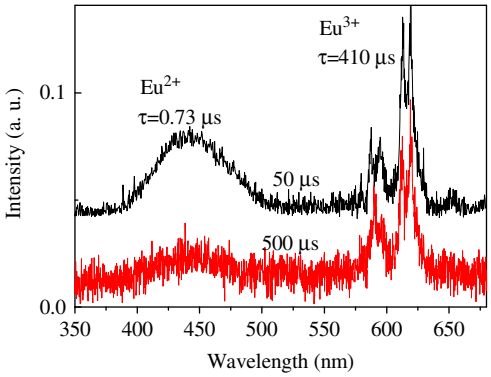

Fig. 7. Time-resolved spectra of $BaCa_2Al_8O_{15}$:xEu^{2+} (x=0.05) nanophosphors measured at different delay times after the pulsed laser excitation at 50 and 500 μs.

displayed by the time resolved spectra in Fig. 7 although its emission intensity is so weak. Eu^{2+} and Eu^{3+} ions show the very different lifetimes, therefore, the time resolved spectra can separate their emission by the time resolved spectra. Under the long delay times, the emission transitions $^5D_0 \rightarrow {}^7F_{1,2}$ from Eu^{3+} ions can be observed in Fig. 7. This indicates that actually two different valance states, +2, and +3, are available for $BaCa_2Al_8O_{15}$:xEu^{2+} (x=0.01–0.07) nanophosphors.

It should also be remarked that although the $BaCa_2Al_8O_{15}$:xEu^{2+} samples were obtained in a reduction atmosphere, this reduction could not be completely realized. Under reducing conditions, Eu^{2+} ions can be stable on alkaline earth metal sites. However, when Eu^{2+} ions are heated within a certain temperature range, they may be oxidized as $Eu^{2+} \rightarrow Eu^{3+} + e^-$. Therefore, Eu^{3+} ions can co-exist with Eu^{2+} ions. In addition, the other intrinsic defect centers were also possibly created, for example, cation vacancies (V_{Ba} or V_{Ca}) and oxygen vacancies V_O, created in the host when the calcination was performed in the reducing atmosphere.

These defects act as hole and electron traps where delayed photoemission results from trapping of some of the excited electrons and as well as holes formed in the valence band at these defect states, which then recombine by thermal excitation releasing energy to excite the electronic states of Eu^{2+} yielding long persistent phosphorescence. The detailed defect states and the depth of their energy level will be detected in the next work.

4. Conclusions

The blue-emitting nanophosphors of $BaCa_2Al_8O_{15}$:xEu^{2+} (x=0.01–0.07) were synthesized by the Pechini method, and its luminescence properties were investigated. The nanoparticle has uniform size of 300–500 nm. The nanophosphor can be efficiently excited by the near UV light (350–450 nm), yielding the intense blue emission centered at 440 nm with CIE of (x=0.142, y=0.07). The corresponding Stokes shift of $BaCa_2Al_8O_{15}$:Eu^{2+} is about 4600 cm^{-1}. Under the same conditions, the luminescence intensity of $BaCa_2Al_8O_{15}$:xEu^{2+} (x=0.05) is 1.2 times higher

than BAM:Eu^{2+} (excitation of 365 nm). $BaCa_2Al_8O_{15}$:xEu^{2+} ($x=0.01$–0.07) present obvious afterglow luminescence after the removal of UV excitation. The afterglow curves of $BaCa_2Al_8O_{15}$:xEu^{2+} ($x=0.01$–0.07) follow the sum of two exponential components: initial fast decay (85–262 s) and the long decay of the afterglow (366–1076 s), which are depended on the Eu^{2+} doping levels. Some defects such as Eu^{3+} centers, cation vacancies and oxygen vacancies could act as hole and electron traps attributing to the long last phosphorescence.

Acknowledgment

This work was supported by Mid-career Researcher Program through National Research Foundation of Korea (NRF) grant funded by the Ministry of Education, Science and Technology (MEST) (Project no. 2009-0078682) and by a project funded by the Priority Academic Program Development of Jiangsu Higher Education Institutions (PAPD).

References

[1] C.C. Lin, R.S. Liu, Advances in phosphors for light-emitting diodes, Journal of Physical Chemistry Letters 2 (2011) 1268–1277.
[2] Lei Chen, Cheng-I. Chu, Ru-Shi Liu, Improvement of emission efficiency and color rendering of high-power LED by controlling size of phosphor particles and utilization of different phosphors, Microelectronics Reliability 52 (2012) 900–904.
[3] R.J. Xie, N. Hirosaki, Silicon-based oxynitride and nitride phosphors for white LEDs—a review, Science and Technology of Advanced Materials 8 (2007) 588–600.
[4] Chun Che Lin, Zhi Ren Xiao, Guang-Yu Guo, Ting-Shan Chan, Ru-Shi Liu, Versatile phosphate phosphors $ABPO_4$ in white light-emitting diodes: collocated characteristic analysis and theoretical calculations, Journal of the American Chemical Society 132 (2010) 3020–3028.
[5] S.H. Lee, H.Y. Koo, Y.C. Kang, Characteristics of α′- and β-Sr_2SiO_4:Eu^{2+} phosphor powders prepared by spray pyrolysis, Ceramics International 36 (2010) 1233–1238.
[6] Selvin Yeşilay Kaya, Erkul Karacaoglu, Bekir Karasu, Effect of Al/Sr ratio on the luminescence properties of $SrAl_2O_4$:Eu^{2+}, Dy^{3+} phosphors, Ceramics International 38 (2012) 3701–3706.
[7] J.H. Kim, H.D. Jang, S.K. Kim, H.B. Lee, E.S. Kim, Photoluminescence and photocurrent characteristics of $Sr_{1-x}Ba_xAl_2O_4$:Eu^{2+}, Ni^{2+} phosphors, Ceramics International 38 (2012) S577–S580.
[8] H.S. Roh, I.S. Cho, J.S. An, C.M. Cho, T.H. Noh, D.K. Yim, D.W. Kim, K.S. Hong, Enhanced photoluminescence property of Dy^{3+} co-doped $BaAl_2O_4$:Eu^{2+} green phosphors, Ceramics International 38 (2012) 443–447.
[9] S.H.M. Poort, W.P. Blokoel, G. Blasse, Luminescence of Eu^{2+} in barium and strontium aluminate and gallate, Chemistry of Materials 7 (1995) 1547–1551.
[10] X. Shi, Y. Huang, J. Yan, L. Shi, X. Qiao, H.J. Seo, Photoluminescence properties of blue-emitting phosphor Eu^{2+}-activated $Ca_3ZnAl_4O_{10}$, Journal of Rare Earths 28 (2010) 693–696.
[11] N. Thompson, P. Murugaraj, C. Rix, D.E. Mainwaring, Role of oxidative pre-calcination in extending blue emission of $Sr_4Al_{14}O_{25}$ nanophosphors formed with microemulsions, Journal of Alloys and Compounds 537 (2012) 147–153.
[12] T. Matsuzawa, Y. Aoki, N. Takeuchi, Y. Murayama, A new long phosphorescent phosphor with high brightness, $SrAl_2O_4$:Eu^{2+}, Dy^{3+}, Journal of the Electrochemical Society 143 (1996) 2670–2673.
[13] T. Takeda, K. Takahashi, K. Uheda, H. Takizawa, T. Endo, Crystal structure and luminescence properties of $Sr_2Al_6O_{11}$:Eu^{2+}, Journal of the Japan Society of Powder and Powder Metallurgy 49 (2002) 1128–1133.
[14] T. Katsumata, K. Sasajima, T. Nabae, S. Komuro, T. Morikawa, Characteristics of strontium aluminate crystals used for long-duration phosphors, Journal of the American Ceramic Society 81 (1998) 413–416.
[15] Y.C. Kang, H.S. Roh, H.D. Park, S.B. Park, Optimization of VUV characteristics and morphology of $BaMgAl_{10}O_{17}$:Eu^{2+} phosphor particles in spray pyrolysis, Ceramics International 29 (2003) 41–47.
[16] A. Nag, T.R.N. Kutty, Role of B_2O_3 on the phase stability and long phosphorescence of $SrAl_2O_4$:Eu, Dy, Journal of Alloys and Compounds 354 (2003) 221–231.
[17] Daniel B. Bem, F.B. Dejene, A.S. Luyt, H.C. Swart, Luminescence studies of a combustion-synthesized blue–green $BaAl_xO_y$:Eu^{2+},Dy^{3+} nanoparticles, Physica B: Condensed Matter 407 (2012) 1561–1565.
[18] M.A. Lephoto, O.M. Ntwaeaborwa, Shreyas S. Pitale, H.C. Swart, J.R. Botha, B.M. Mothudi, Synthesis and characterization of $BaAl_2O_4$:Eu^{2+} co-doped with different rare earth ions, Physica B: Condensed Matter 407 (2012) 1603–1606.
[19] H.C. Swart, O.M. Ntwaeaborwa, P.D. Nsimama, J.J. Terblans, Surface characterization and luminescent properties of $SrAl_2O_4$:Eu^{2+}, Dy^{3+} nano thin films, Physica B: Condensed Matter 407 (2012) 1660–1663.
[20] D. Haranath, V. Shanker, H. Chander, P. Sharma, Tuning of emission colours in strontium aluminate long persisting phosphor, Journal of Physics D: Applied Physics 36 (2003) 2244–2248.
[21] T. Katsumata, R. Sakai, S. Komuro, T. Morikawa, H. Kimura, Growth and characteristics of long duration phosphor crystals, Journal of Crystal Growth 198–199 (1999) 869–871.
[22] K.T. Lee, P.B. Aswath, Synthesis of hexacelsian barium aluminosilicate by a solid-state process, Journal of the American Ceramic Society 83 (2000) 2907–2912.
[23] C. Panatarani, I. Wuled Lenggoro, N. Itoh, H. Yoden, K. Okuyama, Polymer-supported solution synthesis of blue luminescent $BaMgAl_{10}O_{17}$:Eu^{2+} particles, Material Science Engineering: B 122 (3) (2005) 188–195.
[24] Z.Q. Gao, Z.H. Li, P.F. Xia, M.S. Wong, K.W. Cheah, C.H. Chen, Efficient deep-blue organic light-emitting diodes: arylamine-substituted oligofluorenes, Advanced Functional Materials 17 (2007) 3194–3199.
[25] Koen Van den Eeckhout, Philippe F. Smet, Dirk Poelman, Persistent luminescence in Eu^{2+}-doped compounds—a review, Materials 3 (2010) 2536–2566.
[26] Mitsuo Yamaga, Yuki Masui, Shu Sakuta, Nobuhiro Kodama, Keiko Kaminaga, Radiative and nonradiative decay processes responsible for long-lasting phosphorescence of Eu^{2+}-doped barium silicates, Physical Review B 71 (2005) 205102–205108.
[27] Suyin Zhang, Yosuke Nakai, Taiju Tsuboi, Yanlin Huang, Hyo Jin Seo, Luminescence and microstructural features of Eu-activated $LiBaPO_4$ phosphor, Chemistry of Materials 23 (2011) 1216–1224.